The adipokinetic hormones and their cognate receptor from the desert locust, *Schistocerca gregaria*: solution structure of endogenous peptides and models of their binding to the receptor

Graham E. Jackson[1], Elumalai Pavadai[1,2], Gerd Gäde[3] and Niels H. Andersen[4]

[1] Department of Chemistry, University of Cape Town, Cape Town, South Africa.
[2] Current address: Department of Physiology and Biophysics, Boston University School of Medicine, 700 Albany Street, Boston, MA, USA
[2] Department of Biological Sciences, University of Cape Town, Cape Town, South Africa
[3] Chemistry Department, University of Washington, Seattle, Washington, United States

Corresponding Author:
Graham E. Jackson[1]
Private Bag, Rondebosch, Cape Town, 7701, South Africa.
Email address: graham.jackson@uct.ac.za

Abstract

Background. Neuropeptides exert their activity through binding to G-protein coupled receptors (GPCRs). GPCRs are well-known drug targets in the pharmaceutical industry and are being considered as novel targets to control pest insects. Here we investigate the neuropeptide adipokinetic hormone (AKH) system of the desert locust *Schistocerca gregaria*. The desert locust is known for its high reproduction, and for forming devastating swarms consisting of billions of individual insects. It is also known that *S. gregaria* produces three different AKHs as ligands but has only one AKH receptor. The AKH system is known to be essential for metabolic regulation, which is necessary for reproduction and flight activity.

Methods. Nuclear magnetic resonance techniques (NMR) in a dodecylphosphocholin (DPC) micelle solution were used to determine the structure of the three AKHs. The primary sequence of the *S. gregaria* AKH receptor (Schgr-AKHR) was used to construct a 3D molecular model. Further, the 3 AKHs were individually docked to the receptor, and dynamic simulation of the whole ligand-receptor complex performed in a model membrane.

Results. Although the three endogenous AKHs of *S. gregaria* have quite different amino acids sequences and chain length (two octa- and one decapeptide), NMR experiments suggested that they all had a turn structure in DPC micelle solution. The human kappa opioid receptor (hκ-OR)

38   was identified as the best template for homology modeling of Schgr-AKHR.   All three AKH
39   peptides were found to have the same binding site on this receptor, interact with similar residues
40   of the receptor and have comparable binding constants. Molecular switches were also identified;
41   the movement of the receptor could be visually shown when the peptides were docked and the
42   receptor activated.
43   **Conclusions**. The study proposes a model of binding of three endogenous ligands to the one
44   existing AKH receptor in the desert locust and paves the way to use such a model for the design
45   of peptide analogs and finally, peptide mimetics, in the search for novel species-specific
46   insecticides based on receptor-ligand interaction.
47
48

49   ## Introduction

50   In 1976 the primary structure of the first metabolic insect neuropeptide was published (Stone et
51   al. 1976). The decapeptide was isolated from the retrocerebral glands (corpora cardiaca) of the
52   migratory (*Locusta migratoria*) and desert (*Schistocerca gregaria*) locusts.   This neuropeptide
53   was functionally paramount in mobilizing lipids, especially during flight episodes and, hence,
54   was classified as an adipokinetic hormone (AKH). Its modern code name is Locmi-AKH-I (for
55   primary structure, see Table 1). Subsequently, in both locust species, a second species-specific
56   AKH octapeptide was found (Gäde et al. 1986; Siegert et al. 1985) (see Table 1). Later, a third
57   AKH, again an octapeptide, was isolated and functionally characterized from *L. migratoria*
58   (Oudejans et al. 1991) (see Table 1). Genome data mining lead to the discovery of a putative
59   fourth AKH in the migratory locust (Veenstra 2014). The sequence of this octapeptide was
60   identical to an AKH, Aedae-AKH, previously cloned from the yellow fever mosquito, *Aedes*
61   *aegypti* (Kaufmann et al. 2009). It was also found in the corpora cardiaca of the alderfly, *Sialis*
62   *lutaria* (Gäde et al. 2009) and the desert locust (Marchal et al. 2018).
63   All these peptides are members of the large AKH/red pigment-concentrating hormone (RPCH)
64   family, which occurs not only in insects and crustaceans, but also evolved in molluscs (Johnson
65   et al. 2014; Li et al. 2016). The AKH gene codes an mRNA that is translated into a pre-
66   propeptide with the following features: a signal peptide is followed immediately by the
67   respective AKH peptide, a glycine amidation site, a dibasic processing site and, C-terminally,
68   another putative peptide of variable length (Gäde & Marco 2013). After cleavage and post-
69   translational modification, the structure of the mature AKH is characterized by a chain length of
70   8 to 10 amino acids, a pyroglutamate residue (pGlu) at the N-terminus and a carboxyamide at the
71   C-terminus. The amino acids Leu, Ile, Val, Tyr or Phe are found at position 2, Asn or Thr at
72   position 3, the aromatic residues Phe or Tyr at position 4, Ser or Thr at position 5, and various
73   amino acids at position 6, 7 and 10. The aromatic Trp is always present at position 8 and Gly at
74   position 9 (Gäde 2004; Gäde 2009).
75   Most insect neuropeptides, including AKHs, exert their activity via binding to G protein-
76   coupled receptors (GPCRs). In the pharmaceutical industry GPCRs are well known drug targets,
77   and insect neuropeptide GPCRs are being considered as targets for the control of pest insects

78 (Audsley & Down 2015; Verlinden et al. 2014). A number of AKH receptors have been cloned
79 and sequenced (Alves-Bezerra et al. 2016; Caers et al. 2012; Hou et al. 2017, to name a few) and
80 the AKH system with its primarily metabolic function has been identified as a putative target as
81 well (Gäde & Goldsworthy 2003).   With this aim, recent studies (Marchal et al. 2018)
82 characterized the AKHR from the desert locust and used a mammalian cell-based
83 bioluminescence assay to investigate activation of the cloned receptor by a number of naturally-
84 occurring peptides (Marchal et al. 2018).
85 The first 3D-structure of an AKH hormone peptide derived from nuclear magnetic resonance
86 (NMR) spectroscopy was published by Zubrzycki and Gäde in 1994 (Zubrzycki & Gade 1994).
87 Modeling of binding of members of the AKH/RPCH family to their cognate receptors has also
88 been undertaken before: one model has been proposed for an insect, the malaria mosquito,
89 *Anopheles gambiae* (Mugumbate et al. 2013) and another for a crustacean, the water flea
90 *Daphnia pulex* (Jackson et al. 2018). Although the receptors share spatial regions, the binding
91 modes of the two ligands have different orientation (Jackson et al. 2018). In both cases, however,
92 the receptor has only one endogenous, octapeptide ligand. In the current study, three AKH
93 neuropeptides (one decapeptide and two octapeptides, see Table 1) are present in *S. gregaria*;
94 two of these peptides have been found to be active in lipid mobilization (Gäde 1990) and two of
95 these peptides bind to the same receptor (Marchal et al. 2018).   The challenge, hence, was to
96 understand how such different peptides could all activate the same receptor. The available
97 information on the peptides and the AKH receptor of *S. gregaria*, gives us the opportunity to
98 model the binding of these three peptides to their cognate receptor.   This information could then
99 be used to explain how the different peptides are able to activate the same receptor. This step is
100 necessary in order to design novel peptidomimetic agonist or antagonists, which can be
101 synthesize and tested as cheap pest insect control substances.
102
103

Materials & Methods
105 Schgr-AKH-II was synthesized by GL Biochem Ltd (Shanghai, China), Aedae-AKH by Pepmic
106 Co.,Ltd. (Suzhou, China) and Locmi-AKH-I by Peninsula Laboratories (Belmont, California,
107 USA). Purity was checked with HPLC-MS and it was found to be > 95 to 98% pure.   The
108 peptides were not sufficiently soluble in water for the NMR experiments and so solutions were
109 prepared in 30% dimethylsulfoxide (DMSO) and/or in a dodecylphosphocholin (DPC) micelle
110 solution. Typically, 1 mg of sample was dissolved in 0.5 ml of either 20 mM phosphate buffer +
111 30% DMSO or 10:1 (v/v) $H_2O:D_2O$ solution which was 150 mM in deuterated DPC-d38
112 (Cambridge Isotopes, 98.6% d) and buffered with 20 mM potassium phosphate buffer. Peptide–
113 peptide interactions were minimized by maintaining a peptide to micelle ratio of 1:3, assuming
114 50 molecules of DPC per micelle (Jackson et al., 2018). Sodium 4,4-dimethyl-4-silapentane-1-
115 sulfonate (DSS) was used as an internal standard.
116 Nuclear magnetic resonance (NMR) experiments were performed on either, a Bruker Advance
117 700 MHz spectrometer or a Bruker Advance 600 MHz spectrometer with a prodigy probe.   A
118 mixing time of 60 ms was used for Total Correlation Spectroscopy (TOCSY) (Hwang & Shaka
119 1995). A mixing time of 150 ms was used for nuclear Overhauser spectroscopy (NOESY)

120   (Braunschweiler & Ernst 1983). Spectral assignments were based on the method of Wüthrich

121   (Weber et al. 1988; Wüthrich 1986). ^{13}C assignments were based on Heteronuclear Single

122   Quantum Coherence (HSQC) spectra (Sklenar et al. 1993).

123

124   *Peptide molecular dynamics (MD)*

125   The three AKH peptides were built using Maestro [Schrödinger, Inc., New York, NY, USA] and

126   energy minimized using a steepest descent algorithm. NMR restrained molecular dynamic

127   simulations in vacuum, water and DPC were performed using GROMACS version 5.1.2 (Van

128   Der Spoel et al. 2005). Although only the final results in DPC micelle solution are relevant to

129   the current study, the three different environments were used to adequately search

130   conformational space in a reasonable amount of time. Thus, the vacuum simulation was done at

131   600 K to allow the peptide to move faster and overcome any conformational barriers. All

132   simulations were performed using the OPLS-AA all–atom force field with a time step of 2 fs.

133   The LINCS algorithm was used to constraint all bonds. A cut-off of 1.0 nm was used for van

134   der Waals interactions and electrostatic interactions for real space calculations. Vacuum

135   simulations were first done to search conformational space by collecting 100 snapshots of the

136   trajectory during a 10 ns simulation, at 600 K. Each conformation was then annealed to 300 K

137   over 40 ps. Cluster analysis of the resulting structures, using the linkage algorithm of

138   GROMACS and a cut-off of 0.1 nm on the backbone atoms, gave one single large cluster. The

139   conformer in the cluster with the lowest energy was used for simulations in water. Using the

140   tip4p water model, a box containing the peptide and ~7000 water molecules was constructed.

141   Following equilibration, molecular dynamics was performed for 10 ns at 300 K under NPT

142   conditions. In total, 200 structures were collected at 50 ps intervals. Cluster analysis was

143   performed as before and the results used in the DPC/water simulations.

144   For simulations in a water/DPC mixture, the lowest energy structure obtained previously was

145   placed in the center of a 7 nm cubic box filled with ~10 000 SPC water molecules and a 52 DPC

146   molecule micelle as obtained from Tieleman et al.(Tieleman et al. 2000) The micelle was

147   translated so that the center of the micelle was at the bottom edge of the box. This meant that,

148   using periodic boundary conditions, half the micelle was at the bottom of the box and the other

149   half was at the top. The peptide was then placed in the center of the box. Energy minimization

150   was carried out using the steepest descent method to a tolerance of 10 kJ mol^{-1} or to machine

151   precision. Two stages of system equilibration were performed to solvate the peptide and to

152   achieve a steady state starting temperature, pressure and density. The first stage of equilibration

153   involved performing MD for 100 ps under NVT conditions at 300 K followed in the second stage

154   by a further 1 ns MD under NPT conditions. The final MD simulation was for 10 ns during

155   which 200 snapshots were collected. Cluster analysis was performed in the same manner as

156   before.

157

158   *Homology modeling*

159   The primary sequence of the adipokinetic hormone receptor from *S. gregaria*, Schgr-AKHR, was
160   obtained from the GenBank (GenBank ID: AVG47955.1). Transmembrane (TM) helix
161   predictions were computed on-line using PSIPRED (http://bioinf.cs.ucl.ac.uk/psipred/) (Jones
162   2007; Jones et al. 1994; Nugent & Jones 2009). The results showed that this sequence had seven
163   TM helices (Figure S1).

164   The GPCR-ModSim Web server (http://gpcr-modsim.org/) (Rodríguez et al. 2012) was used for
165   template selection and preliminary sequence alignment of Schgr-AKHR. This server accepts an
166   amino acid sequence as input and searches templates by multiple sequence alignments with the
167   query sequence. GPCR-ModSim identified the human kappa opioid receptor (hκ-OR) (PDB ID:
168   4DJH; Wu et al., 2012) as the best template. Subsequently, the sequence alignment between
169   Schgr-AKHR and hκ-OR was manually edited to remove gaps in the transmembrane domains
170   without disrupting their conserved regions. Finally, homology models for Schgr-AKHR were
171   constructed using Modeler 9v7. This is an automated homology modeling program that
172   performs automated protein homology modeling and loop modeling for the receptor by
173   satisfaction of spatial restraints (Sali 1995). The quality of the selected model was evaluated for
174   internal consistency and reliability, such as stereochemical quality, using PROCHECK
175   (Laskowski et al. 1996). The quality of the non-bonded atom interactions was evaluated using
176   ERRAT (Colovos & Yeates 1993a).

177   *Docking studies*
178   The validated Schgr-AKHR model and the structure of the DPC micellar structure of the 3 AKH
179   peptides were prepared for docking simulations using *Protein Preparation Wizard* and *LigPrep*
180   of the Schrödinger suite (Schrödinger Inc., New York, NY, USA). Site-directed mutagenesis
181   studies (Kooistra et al. 2013), molecular modeling and structural analyses (Li et al. 2010)
182   suggest that most of the class A GPCRs share a similar binding pocket *c.f.* retinal bound to
183   rhodopsin, carazolol bound to beta-2 adrenergic receptor (Vilar et al. 2011) and Anoga-HrTH
184   bound to the AKH receptor of *A. gambiae* (Mugumbate et al. 2011).   Thus, the extra-cellular
185   portion of the receptor was used for the docking simulations.
186   *GLIDE docking* (Trott & Olson 2010) was used for peptide docking with a grid space of 72 x 72
187   x 72, which covered all extracellular loops and helices. The receptor grid was generated for
188   peptide ligands and the docking precision was SP-Peptides. This setting automatically increases
189   the number of poses collected.
190
191   *MD of docked structure*
192   The best poses from the docking studies were used as starting structures for a 2 μs molecular
193   dynamics simulation in a 1-palmitoyl-2-oleoyl-glycero-3-phosphocholine (POPC) membrane.
194   Using the CHARMM-GUI [www.charm-gui.org] the docked complex was placed in a POPC
195   membrane (128 POPC molecules) such that it spanned the membrane. The construct was then
196   converted to an OPLS-AA, all–atom, force field. Using GROMACS, ~12000 water molecules
197   were added and the charge neutralized by adding 19 Cl⁻ ions. Several steps of equilibration were

198   used, to pack the membrane around the receptor. This was followed by 1 μs of NPT simulation
199   at 300 K with Berendsen pressure coupling (Berendsen et al. 1984) and a tau-p of 2.0. The free
200   energy of binding of the final structures, from the dynamic simulations, were calculated using
201   Prime-MM-GBSA (Schrödinger Inc., New York, NY, USA).

202

203   **Results**

204   *Spectral assignment*

205   The chemical shift assignments of the three AKH ligands in DPC are given in Tables 2 – 4.
206   Previously, Berjanskii & Wishart (Berjanskii & Wishart 2006) as well as Tremblay (Tremblay
207   2010) have shown that the chemical shifts of peptides are sensitive to the secondary structure and
208   flexibility of the polypeptide. Structuring-induced chemical shift changes (observed shifts
209   minus random coil reference values) were analyzed using the CSDb algorithm available at
210   andersenlab.chem.washington.edu/CSDb/about.php (Eidenschink et al. 2009; Fesinmeyer et al.
211   2004). Figures 1 a-c show such plots for the three ligands. For Schgr-AKH-II both H^N and H_α
212   are shifted up-field, while for Locmi-AKH-I and Aedae-AKH, only the H^N deviations are up-
213   field. The H_α deviations are small and random. It has been shown that polypeptides with a
214   helical structure have, H^N and H_α chemical shifts which are, on average, −0.30 ppm less than
215   their random coil values, while β-sheet structures have shifts of ca. 0.6 ppm (Szilágyi 1995).
216   Thus, each of these peptides has a β-turn structure. Similar results were found for a number of
217   other deca- and octapeptidic members of the AKH family, i.e. for Declu-CC, Melme-CC and
218   Dappu-RPCH (Jackson et al. 2018). However, downfield shifts were previously found for
219   Anoga-HrTH from the *Anopheles* mosquito (Mugumbate et al. 2011; Mugumbate et al. 2013).
220   Using the Random Coil Index tool (Tremblay 2010), the chemical shifts were also used to
221   estimate the model-free order parameter, S^2, of the peptides (see Figure 1d). An order parameter
222   of 1 means the peptide is rigid, while an order parameter of 0 means the peptide has no structure.
223   Figure 1d shows that Locmi-AKH-I is very ordered, with a maximum order parameter of 0.9
224   around proline, whereas the C-terminal has less ordering ($S^2 = 0.30$). On the other hand, Schgr-
225   AKH-II and Aedae-AKH are much more flexible. The order parameter for these two peptides
226   range from 0.1 to 0.4, which is similar to that of Dappu-RPCH, an AKH peptide member from
227   the crustacean water flea (Jackson et al. 2018).
228

229   *MD simulation with DPC micelle*

230   Figure 2 shows the solution structures of the 3 AKH ligands in DPC micelle solution. In each
231   case, the molecular dynamics was started with the peptide in water, but they rapidly diffused to
232   interact with the DPC micelle. Depending on the starting orientation of the peptide relative to
233   the micelle, the peptide would make contact with the phospholipid and move away until a stable
234   orientation was established. This is shown in Figure 3 where the peptide/DPC contact area is
235   plotted as a function of time. For Locmi-AKH-I, contact between the DPC and micelle is
236   established during the equilibration period, for Aedae-AKH it is established after 30 ns, while for

237   Schgr-AKH-II, even after 60 ns the peptide is still not permanently attached to the micelle. It is
238   interesting to note that the contact area between Locmi-AKH-I is much higher than that for the
239   other two peptides and Locmi-AKH-I is much more rigid even though it is longer, a decapeptide
240   versus an octapeptide. The interaction between the peptides and the lipid surface, as shown by
241   the contact area, is important as it has been postulated that, before the ligand binds to its receptor,
242   it first binds to the cell membrane surface.   Thus, surface binding is an important step in receptor
243   activation.
244   In order to show how the structure of the peptides changed during the molecular dynamics, an
245   overlay of each peptide is shown in Figure 2a, b and c. Cluster analysis of the trajectory gave a
246   single large cluster for each peptide with a number of smaller, high energy, clusters. The root
247   conformer and an overlay of each cluster is shown in Figure 2. The predominant conformation
248   of each peptide does have a turn feature but the details differ for each AKH. Locmi-AKH-I (Fig.
249   2a) has a clear β-turn around its proline residue; Aedae-AKH (Fig. 2b) has a more open structure
250   compared to the other peptides and no marked turn around proline; Schgr-AKH-II (Fig. 2c) is
251   tightly coiled in DPC solution.
252
253   *Receptor Construct*
254   Use of the GPCR-ModSim server gave the crystal structure of the hκ-OR (PDB ID: 4DJH), with
255   2.9 Å resolution, as a top template for Schgr-AKHR. The crystal structure has the selective
256   antagonist JDTic complexed to the receptor (Hu et al., 2012). This template has the highest
257   sequence identity (26.33%) compared to other templates as shown in Figure S2.   hκ-OR belongs
258   to the class A (rhodopsin-like), γ-subfamily of G-protein-coupled receptors (GPCRs) and was
259   selected to build models for Schgr-AKHR. The initial sequence alignment from the GPCR-
260   ModSim server was aligned manually with the use of Chimera (Pettersen et al. 2004a; Pettersen
261   et al. 2004b)). The predicted transmembrane helices of Schgr-AKHR and the PDB structural
262   assignments of hκ-OR were also used to confirm the alignment as shown in Figure S1. The
263   sequence analysis shows that the conserved residues in the seven TM helices (TM1-TM7) of hκ-
264   OR are also highly conserved within Schgr-AKHR (conserved residues highlighted by purple
265   coloured boxes in Figure S1), indicating that they may be involved in functions, such as
266   signaling and ligand binding, of Schgr-AKHR. Additionally, as in hκ-OR, disulfide forming
267   cysteine residues (Cys-131 and Cys-210) are conserved in Schgr-AKHR. The predicted TM
268   helices of Schgr-AKHR (Figure S3) are consistent with the TM helices of hκ-OR: there are no
269   gaps or insertions in these regions, signifying that the target sequence is correctly aligned with
270   the template sequence and, hence, can be used for the modeling process.
271   The homology models of Schgr-AKHR were built using the *Modeler* 9v7 program. The input
272   parameters of *Modeler* were set to generate 100 models with high structural optimization. A
273   disulfide bridge, Cys-131–Cys-210, was defined as in the template structure. The best model was
274   selected based on the lowest PDF (molecular probability density function) energies and DOPE
275   score (discrete optimized protein energy) for the docking simulations. The selected models'
276   qualities were subsequently assessed with structural evaluation programs such as PROCHECK

277   and ERRAT. Ramachandran plot analyses of the Schgr-AKHR model from PROCHECK are
278   shown in Figure S4. All the residues were either in favored or in allowed regions, indicating that
279   the backbone torsion angles (phi and psi) of this model are reliable. In addition, the ERRAT
280   score, so-called overall quality factor, was computed on the Schgr-AKHR model to check the
281   quality of its non-bonded atomic interactions. The normally accepted score range for a high-
282   quality model is >50 (Colovos & Yeates 1993b). The ERRAT score for the Schgr-AKHR model
283   was 78, showing that the model is within the high-quality range. All these validation methods
284   demonstrated that the model is reliable and can be used for further studies. The final 3D
285   structure of the Schgr-AKHR model, as shown in Figure S5A, is similar in overall fold with the
286   template protein hκ-OR (Fig. S5B). The superposition of the Schgr-AKHR model with that of
287   hκ-OR displayed a 2.804 A˚ root mean squared deviation (RMSD) for 1332 atoms pairs. This
288   low RMSD demonstrates that the overall tertiary structure of the model are similar to the
289   template structure. In addition, the superimpositions indicate that the seven transmembrane
290   helices are highly conserved with hκ-OR. However, there are slight structural variations in the
291   loop regions of the model.
292
293   *Ligand Docking*
294   LigPrep was used to generate multiple conformers of the three AKH peptides, which were then
295   docked to the Schgr-AKHR model. A receptor grid was generated for the extra-cellular half of
296   the GPCR and the peptide docked using SP-Peptide precision. One hundred different poses were
297   collected and scored for each peptide. An overlay of the highest scoring poses gave the same
298   receptor binding site for all three peptides. This binding pocket consisted of a cleft running
299   across the top of Schgr-AKHR, between helices 2, 6 and 7 and extra-cellular loops 2 and 4
300   (details shown in Figures 4 – 6). The peptides lay along this cleft. It was found that, while the
301   GLIDE protocol tried to dock many different conformations of the peptide, only those with some
302   turn structure were successful. Many of the docked poses had similar GLIDE scores but
303   different sets of peptide/receptor interactions.   During the docking, it was found that the
304   orientation of the peptide within the binding pocket did not change. For this reason, the docking
305   was repeated with the peptide rotated through 180 degrees around the axis of the transmembrane
306   helices i.e., the direction of N-terminus to the C-terminus was reversed.   Again, the peptide
307   could be docked successfully, indicating that the binding pocket was quite promiscuous.
308   Although either orientation of the peptide would bind to the receptor, the binding energies of the
309   two orientations differed by some 50 kcal/mol and hence the original orientation was chosen for
310   further study.
311   The docked structure of each AKH peptide with the highest binding energy, was used as the
312   starting structure for molecular dynamics of the complex in a POPC membrane. During the
313   dynamics, the ligands were found to move, and individual side-chains rotate within the binding
314   site, making and breaking H-bonds to various residues of the receptor. This was essentially the
315   same as what was found during the GLIDE docking.   While the POPC membrane added to the
316   computational cost of the simulation, it was necessary to prevent the trans-membrane helices of

317 the receptor from moving apart.   Snapshots of the simulation were transferred to Maestro, where
318 Prime-MM-GBSA was used to calculate the binding energy.
319 Figure 4a and b shows an overlay of several snapshots of the dynamic simulation of the
320 octapeptide, Schgr-AKH-II, in its receptor binding pocket.   As can be seen, the overall
321 conformation of Schgr-AKH-II remains the same (Figure 4c) but the side-chains move within the
322 binding site, forming and breaking intra- and inter-molecular H-bonds. There is also some
323 movement of the receptor during the dynamics. The free energy of binding of the different
324 snapshots were not significantly different and ranged from -94 to -116 kcal/mol over the 1 μs
325 simulation.
326 The bound conformation of Schgr-AKH-II is shown in Figure 4c, while Figure 4d is an overlay
327 of bound Schgr-AKH-II and its lowest energy conformation in DPC micelle solution. The
328 agreement of these two conformers is remarkable, especially considering that the GLIDE – SP
329 protocol generates some 100 different starting conformations for the peptide docking.
330 Figure 5a shows the bound conformation of Locmi-AKH-I, while Figure 5b is an overlay of this
331 bound conformer and the lowest energy conformer found in DPC micelle solution. The
332 agreement here is not as close as that for Schgr-AKH-II, but the same turn structure is seen.
333 Figure 5c shows Locmi-AKH-I in the receptor binding pocket, while Figures 5d and e show the
334 details of how Locmi-AKH-I fits into the receptor: the decapeptide stretches across the cleft in
335 the receptor with the central portion of the peptide fitting into the binding pocket, but the two
336 termini pointing outside the binding pocket. Locmi-AKH-I gave the most trouble during the
337 docking stage as poses were frequently rejected. During the molecular dynamics, the terminal
338 amide of this decapeptide was sometimes found to H-bond to a POPC molecule, which is of
339 course not present during the GLIDE docking. The final binding energy for Locmi-AKH-I was -
340 98 kcal/mol.
341 Figure 6a and b show how Aedae-AKH fits into the binding pocket of the Schgr-AKHR model.
342 The arrangement is similar to that of Locmi-AKH-I, except, in this case, the termini do not
343 extend outside the receptor.   In the case of Aedae-AKH, ECL4 folds over the top of the binding
344 site, trapping the peptide inside. The conformation of bound Aedae-AKH is shown in Figure 6c,
345 and an overlay with the DPC micelle solution conformation is shown in Figure 6d. Again, these
346 two conformations are very similar, supporting the idea that the peptides are pre-arranged on the
347 cell surface.   The binding energy of Aedae-AKH was -88 kcal/mol.
348 Ligand interaction diagrams for the three ligands are shown in Figure 7, while Table 5 lists the
349 interactions between the ligands and Schgr-AKHR.   From these data, it is clear that all three
350 AKH ligands have very similar interactions with Schgr-AKHR. Both Schgr-AKH-II and Aedae-
351 AKH, H-bond to His169 of the receptor, while W^8 of Locmi-AKH-I π-stacks with this residue.
352 In Locmi-AKH-I, the amide carbonyl, pE^1CO, H-bonds to Lys281, while in Aedae-AKH it is
353 $pE^1O_{\varepsilon 1}$ which H-bonds to Lys281. The terminal residue of both Schgr-AKH-II and Locmi-AKH-
354 I H-bond to Lys288.
355
356 *Analysis of molecular switches*

357 A feature of class A GPCRs is the presence of highly conserved molecular switch motifs.   These
358 switches, which play key roles in the stabilization of the receptor in an inactive and active state,
359 include a TM3-6 lock, a SPLF switch, a tyrosine toggle and a DRY ionic lock. The breaking of
360 these switches results in movement of the transmembrane helices, which can activate the
361 receptor (Trzaskowski et al. 2012). These switches are the same as those reported for the AKH
362 receptor of *Drosphilia melanogaster*, *Tribolium castaneum, A. gambiae* and *Rhodnius prolixus*
363 (Rasmussen et al. 2015), suggesting that the activation mechanism of Schgr-AKHR may be the
364 same.
365 The DRY ionic lock between arginine and tyrosine is postulated to open and close during
366 receptor activation. This is shown in Figure 8. In the inactive state, the DRY switch is closed
367 (Figure 8b) but upon ligand binding, TM6 and TM3 twist, opening this switch (Figure 8c).
368 The TM3-6 lock involves two residues in the binding pocket, Arg^{107} on TM3 and Tyr^{265} on TM6
369 (Figure 9a).   In the inactive state these two residues are far apart, but on ligand activation, they
370 move closer together. Fig 9a also shows, in the active state, Arg^{107} H-bonding with Glu^{190} of
371 ECL4.   It was noted before that this loop closes over the binding pocket after ligand binding. In
372 Fig 9a one can also clearly see how TM6 and TM3 move together on the extra-cellular side but
373 move away from each other on the intra-cellular side, upon activation.
374 The tyrosine toggle switch involves the NPxxY motif on TM7 and Tyr^{213} on TM5 (Fig 9b).
375

Discussion

377 As has been found before, insect neuropeptides are flexible in solution but generally have a
378 preferred β-turn conformation (Mercurio et al. 2018; Shen et al. 2018; Zubrzycki 2000). Using
379 CD spectroscopy, Cusinato *et al*. (Cusinato et al. 1998) proposed a P II extended conformation
380 for the AKH/RPCH peptides, at low temperatures, in aqueous solution.   However, they found
381 that the majority of AKH/RPCH peptides adopted a β-turn conformation in the presence of 0.6%
382 SDS. This is what was found in DPC micelle solution by both NMR chemical shift and
383 molecular modeling results for the three peptides Schgr-AKH-II, Aedae-AKH and Locmi-AKH-I
384 in the current study. These peptides are not very soluble in water but are readily soluble in DPC
385 micelle solution, which is a clear indication that they interact with the micelle. Previously, using
386 DOSY NMR spectroscopy, we showed that the crustacean AKH member, Dappu-RPCH, binds
387 to the micelle in DPC solution, and that the micelle consists of ~ 50 DPC molecules (Jackson et
388 al. 2018).   This was also shown by the molecular modeling for the 3 locust peptides in the
389 present study.   Locmi-AKH-I interacted strongly with the micelle and perhaps this is the reason
390 why this peptide had a much higher order parameter than the other two peptides.
391 Despite chain length and sequence differences, all three peptides were found to have the same
392 binding site on the receptor. They all had similar binding constants and interacted with the same
393 receptor residues. This is in agreement with previous results of Marchal *et al*. (Marchal et al.
394 2018) where many members of the AKH family activated Schgr-AKHR *in vitro,* to the same
395 extent and it was concluded that this receptor was quite promiscuous. In the present study,
396 multiple binding poses were found for the peptides in the binding site and this was confirmed by

397   molecular dynamics in a POPC membrane. Here each peptide was found to move within the
398   binding site, interacting with different residues. This may account for the same receptor being
399   activated naturally by all three peptides.   Interestingly, during the molecular dynamics, the
400   receptor itself moved, closing over the binding site and opening up on the intra-cellular side.
401   This motion has been postulated to result in receptor activation, with a G-protein able to bind to
402   the more open receptor.   Figure 8a, which is an overlay of the active and inactive receptor,
403   shows this movement of the helices. Measurements show that Ala-243, on TM6, moves some
404   6.4 Å on receptor activation. One can also see that ECL6 and ECL4 (Figure 4b) close over the
405   binding site.
406   It is interesting to compare and contrast the binding of Schgr-AKH-II, Aedae-AKH and Locmi-
407   AKH-I with the binding of a crustacean red pigment-concentrating hormone from *Daphnia*
408   *pulex*, Dappu-RPCH, to its cognate receptor, Dappu-RPCHR (Jackson et al. 2018). Both
409   receptors have similar binding sites involving TM2, 6 and 7 but Dappu-RPCHR also uses
410   extracellular loops 1, 2 and 3, while Schgr-AKHR involves loops 2 and 4 (and loop 6 in the
411   active receptor). Dappu-RPCH undergoes significant conformational changes upon receptor
412   binding, having a more extended structure in solution but a more pronounced β-turn when
413   bound. On the other hand, Schgr-AKH-II, Aedae-AKH and Locmi-AKH-I, undergo very little
414   conformational change upon receptor binding. This might account for the higher binding
415   constant of these three peptides relative to Dappu-RPCH. The similarity between the
416   AKH/RPCH systems is understandable given the evolution of the AKH/corazonin/ACP/GnRH
417   receptor superfamily and their ligands. (Hauser & Grimmelikhuijzen 2014)
418   The presented model of Schgr-AKHR can be compared to another class A GPCR, the human
419   gonadotropin releasing hormone receptor, GnRHR (Flanagan & Manilall 2017).   This receptor
420   has an exaggerated bend around Pro, in a CWxPY motif found on TM6. In GnRHR, this bend is
421   stabilized by a water mediated H-bond between Cys[47] and Tyr[51] on TM6 of the CWxPY motif
422   and by H-bonding to a residue in TM7. The presented model of Schgr-AKHR also has this
423   CWxPY motif in TM6, which results in a proline kink. In the active receptor, Cys and Tyr
424   residues are correctly oriented for water mediated H-bonding, with a distance of 3.18 Å between
425   them. Also, Trp[262] of the CWxPY motif was found to H-bond to Asn[297] of TM7.   The
426   functional importance of this motif was demonstrated by mutations associated with congenital
427   hypogonadotropic hypogonadism (CHH). This rare disorder results from decreased production
428   or secretion of gonadotropin-releasing hormone (GnRH) and/or lack of action of GnRH upon
429   GnRHR.   There are some 25 genes identified in this condition, but if the Pro residue is
430   substituted by Arg, there is complete disruption of the receptor function. This shows the
431   importance of this proline kink. On the other hand, when the Cys of this receptor motif is
432   mutated to Tyr or Ala, the GnRH ligand does not bind to the receptor (Flanagan & Manilall
433   2017).   Interestingly, in the inactive Schgr-AKHR, there was a H-bond between Trp-CO and
434   Tyr-NH but there was no H-bond between Trp[262] and Asn[297]. Upon ligand binding, however,
435   the helices moved in such a way that the one H-bond broke and the other formed. This is similar
436   to the DRY switch described above. Binding similarities between GnRHR and Schgr-AKHR are

437 not unexpected. It has long been accepted that GnRH and AKH are peptides belonging to the
438 same superfamily because not only are the ligands structurally closely related but also the
439 cognate receptors (Gäde et al. 2011; Hauser & Grimmelikhuijzen 2014; Roch et al. 2011; Roch
440 et al. 2014).
441

Conclusions

443 In this paper, we have shown that the putative receptor, Schgr-AKHR, is a member of the Class
444 A superfamily of G-protein coupled receptors. It has 7 transmembrane helices and the same
445 conserved residues as other AKH receptors. Schgr-AKHR also has a number of molecular
446 switch motifs, which are a feature of class A GPCRs. Our results show that the three
447 endogenous peptides, Schgr-AKH-II, Aedae-AKH and Locmi-AKH-I, all bind to the same
448 receptor binding site and with very similar binding constants.   This may be surprising, as the
449 three ligands are very different; their sequence is different and one is a decapeptide, while the
450 other two are octapeptides. However, *L. migratoria* and *S. gregaria*, have only one AKH
451 receptor so it could be expected that the three endogenous peptides would have to bind to this
452 single receptor. These results also fit previous findings that, *in vitro*, the AKH receptor of *S.*
453 *gregaria* is equally well activated by a number of AKH members.
454

455 The similarities in the ligand binding of Schgr-AKHR and Dappu-RPCH/Dappu-RPCHR
456 supports the evolutionary development of the AKH/corazonin/ACP/GnRH receptor superfamily.
457 The next step in this study would be to use *in silico* screening to identify suitable agonists or
458 antagonists, which could act as next generation insecticides.
459

460

References

462

463 Alves-Bezerra M, De Paula IF, Medina JM, Silva-Oliveira G, Medeiros JS, Gäde G, and Gondim
464 KC. 2016. Adipokinetic hormone receptor gene identification and its role in triacylglycerol
465 metabolism in the blood-sucking insect *Rhodnius prolixus*. *Insect Biochemistry and Molecular*
466 *Biology* 69:51-60. https://doi.org/10.1016/j.ibmb.2015.06.013

467 Audsley N, and Down RE. 2015. G protein coupled receptors as targets for next generation
468 pesticides. *Insect Biochemistry and Molecular Biology* 67:27-37. S0965-1748(15)30030-8 [pii]

469 Berendsen HJC, Postma JPM, van Gunsteren WF, DiNola A, and Haak JR. 1984. Molecular
470 dynamics with coupling to an external bath. *The Journal of Chemical Physics* 81:3684-3690.

471 Berjanskii M, and Wishart DS. 2006. NMR: Prediction of protein flexibility. *Nature Protocols*
472 1:683-688.

473   Braunschweiler L, and Ernst RR. 1983. Coherence transfer by isotropic mixing - Application to
474   proton correlation spectroscopy. *Journal of Magnetic Resononance* 53:521-528.

475   Caers J, Peeters L, Janssen T, De Haes W, Gäde G, and Schoofs L. 2012. Structure-activity
476   studies of *Drosophila* adipokinetic hormone (AKH) by a cellular expression system of dipteran
477   AKH receptors. *General and Comparative Endocrinology* 177:332-337.
478   10.1016/j.ygcen.2012.04.025

479   Colovos C, and Yeates TO. 1993b. Verification of protein structures: Patterns of nonbonded
480   atomic interactions. *Protein Science* 2:1511-1519.

481   Cusinato O, Drake AF, Gäde G, and Goldsworthy GJ. 1998. The molecular conformations of
482   representative arthropod adipokinetic peptides determined by circular dichroism spectroscopy.
483   *Insect Biochemistry and Molecular Biology* 28:43-50. https://doi.org/10.1016/S0965-
484   1748(97)00094-5

485   Eidenschink L, Kier BL, Huggins KNL, and Andersen NH. 2009. Very short peptides with stable
486   folds: Building on the interrelationship of Trp/Trp, Trp/cation, and Trp/backbone amide
487   interaction geometries. *Proteins: Structure, Function, and Bioinformatics* 75:308-322.
488   10.1002/prot.22240

489   Fesinmeyer RM, Hudson FM, and Andersen NH. 2004. Enhanced hairpin stability through loop
490   design: The case of the protein G B1 domain hairpin. *Journal of the American Chemical Society*
491   126:7238-7243. 10.1021/ja0379520

492   Flanagan CA, and Manilall A. 2017. Gonadotropin-releasing hormone (GnRH) receptor structure
493   and GnRH binding. *Frontiers in Endocrinology* 8:274.

494   Gäde G. 1990. Structure–function studies on hypertrehalosaemic and adipokinetic hormones:
495   activity of naturally occurring analogues and some N- and C-terminal modified analogues.
496   *Physiological Entomology* 15:299-316. 10.1111/j.1365-3032.1990.tb00518.x

497   Gäde G. 2004. Regulation of intermediary metabolism and water balance of insects by
498   neuropeptides. Annual Review of Entomology 49:93-113.

499   Gäde G. 2009. Peptides of the adipokinetic hormone/red pigment-concentrating hormone
500   ficalamily. *Annals of the New York Academy of Sciences* 1163:125-136.

501   Gäde G, and Goldsworthy GJ. 2003. Insect peptide hormones: a selective review of their
502   physiology and potential application for pest control. *Pest Management Science* 59:1063-1075.
503   10.1002/ps.755

504   Gäde G, Goldsworthy GJ, Schaffer MH, Cook JC, and Rinehart KL. 1986. Sequence analyses of
505   adipokinetic hormones II from corpora cardiaca of *Schistocerca nitans*, *Schistocerca gregaria*,
506   and *Locusta migratoria* by fast atom bombardment mass spectrometry. *Biochemical and*
507   *Biophysical Research Communications* 134:723-730.

508   Gäde G, and Marco HG. 2013. Chapter 28 - AKH/RPCH Peptides. In: Kastin AJ, ed. *Handbook*
509   *of Biologically Active Peptides (Second Edition)*. Boston: Academic Press, 185-190.

510   Gäde G, Šimek P, and Marco HG. 2009. The first identified neuropeptide in the insect order
511   Megaloptera: A novel member of the adipokinetic hormone family in the alderfly *Sialis lutaria*.
512   *Peptides* 30:477-482.

513   Gäde G, Šimek P, and Marco HG. 2011. An invertebrate [hydroxyproline]-modified
514   neuropeptide: Further evidence for a close evolutionary relationship between insect adipokinetic
515   hormone and mammalian gonadotropin hormone family. *Biochemical and Biophysical Research*
516   *Communications* 414:592-597. https://doi.org/10.1016/j.bbrc.2011.09.127

517   Hauser F, and Grimmelikhuijzen CJP. 2014. Evolution of the AKH/corazonin/ACP/GnRH
518   receptor superfamily and their ligands in the Protostomia. *General and Comparative*
519   *Endocrinology* 209:35-49. 10.1016/j.ygcen.2014.07.009

520   Hou Q-L, Chen E-H, Jiang H-B, Wei D-D, Gui S-H, Wang J-J, and Smagghe G. 2017.
521   Adipokinetic hormone receptor gene identification and its role in triacylglycerol mobilization
522   and sexual behavior in the oriental fruit fly (*Bactrocera dorsalis*). *Insect Biochemistry and*
523   *Molecular Biology* 90:1-13. https://doi.org/10.1016/j.ibmb.2017.09.006

524   Hwang TL, and Shaka AJ. 1995. Water suppression that works. Excitation sculpting using
525   arbitrary wave-forms and pulsed-field gradients. *Journal of Magnetic Resonance, Series A*
526   112:275-279. https://doi.org/10.1006/jmra.1995.1047

527   Jackson GE, Pavadai E, Gäde G, Timol Z, and Andersen NH. 2018. Interaction of the red
528   pigment-concentrating hormone of the crustacean *Daphnia pulex*, with its cognate receptor,
529   Dappu-RPCHR: A nuclear magnetic resonance and modeling study. *International Journal of*
530   *Biological Macromolecules* 106:969-978. https://doi.org/10.1016/j.ijbiomac.2017.08.103

531   Johnson JI, Kavanaugh SI, Nguyen C, and Tsai P-S. 2014. Localization and functional
532   characterization of a novel adipokinetic hormone in the mollusk, *Aplysia californica*. *PLOS One*
533   9:e106014. 10.1371/journal.pone.0106014

534   Jones DT. 2007. Improving the accuracy of transmembrane protein topology prediction using
535   evolutionary information. *Bioinformatics* 23:538-544.

536 Jones DT, Taylor WR, and Thorton JM. 1994. A model recognition approach to the prediction of
537 all-helical membrane-protein structure and topology. *Biochemistry* 33:3038-3049.

538 Kaufmann C, Merzendorfer H, and Gäde G. 2009. The adipokinetic hormone system in
539 Culicinae (Diptera: Culicidae): Molecular identification and characterization of two adipokinetic
540 hormone (AKH) precursors from *Aedes aegypti* and *Culex pipiens* and two putative AKH
541 receptor variants from *A. aegypti*. *Insect Biochemistry and Molecular Biology* 39:770-781.

542 Kooistra AJ, Kuhne S, De Esch IJP, Leurs R, and De Graaf C. 2013. A structural
543 chemogenomics analysis of aminergic GPCRs: Lessons for histamine receptor ligand design.
544 *British Journal of Pharmacology* 170:101-126. 10.1111/bph.12248

545 Laskowski RA, Rullmann JAC, MacArthur MW, Kaptein R, and Thornton JM. 1996. AQUA
546 and PROCHECK-NMR: Programs for checking the quality of protein structures solved by NMR.
547 *Journal of Biomolecular NMR* 8:477-486.

548 Li S, Hauser F, Skadborg SK, Nielsen SV, Kirketerp-Møller N, and Grimmelikhuijzen CJP.
549 2016. Adipokinetic hormones and their G protein-coupled receptors emerged in Lophotrochozoa.
550 *Scientific Reports* 6:32789. 10.1038/srep32789 https://www.nature.com/articles/srep32789 -
551 supplementary-information

552 Li YY, Hou TJ, and Goddard III WA. 2010. Computational modeling of structure-function of G
553 protein-coupled receptors with applications for drug design. *Current Medicinal Chemistry*
554 17:1167-1180. 10.2174/092986710790827807

555 Marchal E, Schellens S, Monjon E, Bruyninckx E, Marco H.G., Gäde G, Vanden Broeck J, and
556 Verlinden H. 2018. Analysis of peptide ligand specificity of different insect adipokinetic
557 hormone receptors. *International Journal of Molecular Science* 19(2) pii E542 doi:
558 10.3390/ijms19020542.

559 Mercurio FA, Scaloni A, Caira S, and Leone M. 2018. The antimicrobial peptides casocidins I
560 and II: Solution structural studies in water and different membrane-mimetic environments.
561 *Peptides*. https://doi.org/10.1016/j.peptides.2018.09.004

562 Mugumbate G, Jackson GE, and van der Spoel D. 2011. Open conformation of adipokinetic
563 hormone receptor from the malaria mosquito facilitates hormone binding. *Peptides* 32:553-559.
564 10.1016/j.peptides.2010.08.017

565 Mugumbate G, Jackson GE, van der Spoel D, Koever KE, and Szilagyi L. 2013. *Anopheles*
566 *gambiae*, Anoga-HrTH hormone, free and bound structure - A nuclear magnetic resonance
567 experiment. *Peptides* 41:94-100. 10.1016/j.peptides.2013.01.008

568 Nugent T, and Jones DT. 2009. Transmembrane protein topology prediction using support vector
569 machines. *BMC Bioinformatics* 10. 10.1186/1471-2105-10-159

570 Oudejans RCHM, Kooiman FP, Heerma W, Versluis C, Slotboom AJ, and Beenakkers AMT.
571 1991. Isolation and structure elucidation of a novel adipokinetic hormone (Lom-AKH-III) from
572 the glandular lobes of the corpus cardiacum of the migratory locust, *Locusta migratoria*.
573 *European Journal of Biochemistry* 195:351-359.

574 Pettersen EF, Goddard TD, Huang CC, Couch GS, Greenblatt DM, Meng EC, and Ferrin TE.
575 2004a. UCSF Chimera - A visualization system for exploratory research and analysis. *Journal of
576 Computational Chemistry* 25:1605-1612. 10.1002/jcc.20084

577 Rasmussen M, Leander M, Ons S, and Nichols R. 2015. Conserved molecular switch interactions
578 in modeled cardioactive RF-NH2 peptide receptors: Ligand binding and activation. *Peptides*
579 71:259-267. 10.1016/j.peptides.2015.07.012

580 Roch GJ, Busby ER, and Sherwood NM. 2011. Evolution of GnRH: Diving deeper. *General and
581 Comparative Endocrinology* 171:1-16. https://doi.org/10.1016/j.ygcen.2010.12.014

582 Roch GJ, Busby ER, and Sherwood NM. 2014. GnRH receptors and peptides: Skating backward.
583 *General and Comparative Endocrinology* 209:118-134.
584 https://doi.org/10.1016/j.ygcen.2014.07.025

585 Rodríguez D, Bello X, and Gutiérrez-de-Terán H. 2012. Molecular modelling of G protein-
586 coupled receptors through the web. *Molecular Informatics* 31:334-341. 10.1002/minf.201100162

587 Sali A. 1995. Comparative protein modeling by satisfaction of spatial restraints. *Molecular
588 Medicine Today* 1:270-277.

589 Shen Z, Jiang X, Yan L, Chen Y, Wang W, Shi Y, Shi L, Liu D, and Zhou N. 2018. Structural
590 basis for the interaction of diapause hormone with its receptor in the silkworm, *Bombyx mori*.
591 *The FASEB Journal* 32:1338-1353. 10.1096/fj.201700931R

592 Siegert K, Morgan P, and Mordue W. 1985. Primary structures of locust adipokinetic hormones
593 II. . *Biological Chemistry Hoppe-Seyler* 366:723-727.

594 Sklenar V, Piotto M, Leppik R, and Saudek V. 1993. Gradient-tailored water suppression for 1H-
595 15N HSQC experiments optimized to retain full sensitivity. *Journal of Magnetic Resononance A*
596 102:241-245.

597 Stone JV, Mordue W, Batley KE, and Morris HR. 1976. Structure of locust adipokinetic
598 hormone, a neurohormone that regulates lipid utilisation during flight. *Nature* 263:207-211.
599 10.1038/263207a0

600   Szilágyi L. 1995. Chemical shifts in proteins come of age. *Progress in Nuclear Magnetic*
601   *Resonance Spectroscopy* 27:325-442. 10.1016/0079-6565(95)01011-2
602
603

604   Tieleman DP, Van Der Spoel D, and Berendsen HJC. 2000. Molecular dynamics simulations of
605   dodecylphosphocholine micelles at three different aggregate sizes: Micellar structure and chain
606   relaxation. *Journal of Physical Chemistry B* 104:6380-6388.

607   Tremblay M-L. 2010. The predictive accuracy of secondary chemical shifts is more affected by
608   protein secondary structure than solvent environment. *Journal of Biomolecular NMR* 46:257.
609   10.1007/s10858-010-9400-5

610   Trott O, and Olson AJ. 2010. Software news and update AutoDock Vina: Improving the speed
611   and accuracy of docking with a new scoring function, efficient optimization, and multithreading.
612   *Journal of Computational Chemistry* 31:455-461. 10.1002/jcc.21334

613   Trzaskowski B, Latek D, Yuan S, Ghoshdastider U, Debinski A, and Filipek S. 2012. Action of
614   molecular switches in GPCRs - Theoretical and experimental studies. *Current Medicinal*
615   *Chemistry* 19:1090-1109. 10.2174/092986712799320556

616   Van Der Spoel D, Lindahl E, Hess B, Groenhof G, Mark AE, and Berendsen HJC. 2005.
617   GROMACS: Fast, flexible, and free. *Journal of Computational Chemistry* 26:1701-1718.

618   Veenstra JA. 2014. The contribution of the genomes of a termite and a locust to our
619   understanding of insect neuropeptides and neurohormones. *Frontiers in Physiology* 5:454.

620   Verlinden H, Vleugels R, Zels S, Dillen S, Lenaerts C, Crabbé K, Spit J, and Vanden Broeck J.
621   2014. Receptors for neuronal or endocrine signalling molecules as potential targets for the
622   control of insect pests. *Advances in Insect Physiology* 46: 167-303.

623   Vilar S, Ferino G, Phatak SS, Berk B, Cavasotto CN, and Costanzi S. 2011. Docking-based
624   virtual screening for ligands of G protein-coupled receptors: Not only crystal structures but also
625   in silico models. *Journal of Molecular Graphics and Modelling* 29:614-623.
626   10.1016/j.jmgm.2010.11.005

627   Weber PL, Morrison R, and Hare D. 1988. Determining stereo-specific 1H Nuclear magnetic
628   resonance assignments from distance geometry calculations. *Journal of Molececular Bioliology*
629   204:483-487.

630   Wüthrich K. 1986. *NMR of Proteins and Nucleic Acids*. New York: Wiley.

631   Zubrzycki IZ. 2000. Molecular dynamics study on an adipokinetic hormone peptide in aqueous
632   solution. *Zeitschrift für Naturforschung C, A Journal of Biosciences* 55:125-128.

633   Zubrzycki IZ, and Gäde G. 1994. Conformational study on an insect neuropeptide of the
634   AKH/RPCH-family by combined 1H-NMR spectroscopy and molecular mechanics. *Biochemical*
635   *and Biophysical Research Communications* 198:228-235.
636   https://doi.org/10.1006/bbrc.1994.1032

637

638

639

Figure 1

NMR chemical shift deviations and model-free order parameters of Schgr-AKH-II, Locmi-AKH-I and Aedae-AKH in DPC micelle solution.

Plots of H_α and H^N random coil chemical shift deviations of: (a) Schgr-AKH-II. (b) Locmi-AKH-I

(c). Aedae-AKH. (d) Model-free order parameter, S^2.
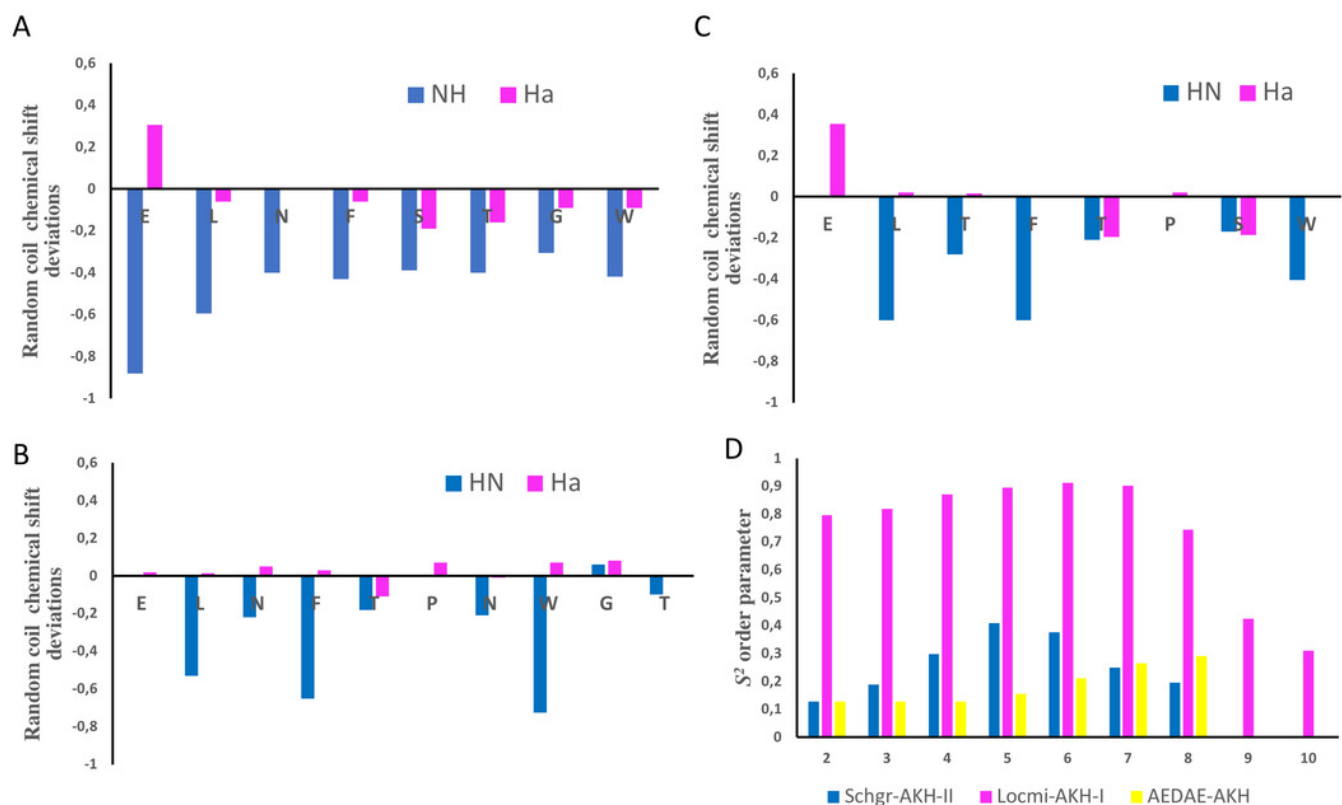
Figure 2

Solution cluster overlay and the root conformation of Schgr-AKH-II, Locmi-AKH-I and Aedae-AKH in DPC micelle solution.

(A) Cluster overlay of Locmi-AKH-I. (B) Root conformer of Locmi-AKH-I. (C) Cluster overlay of Aedae-AKH-I. (D) Root conformer of Aedae-AKH-I. (E) Cluster overlay of Schgr-AKH-II. (F) Root conformer of Schgr-AKH-II
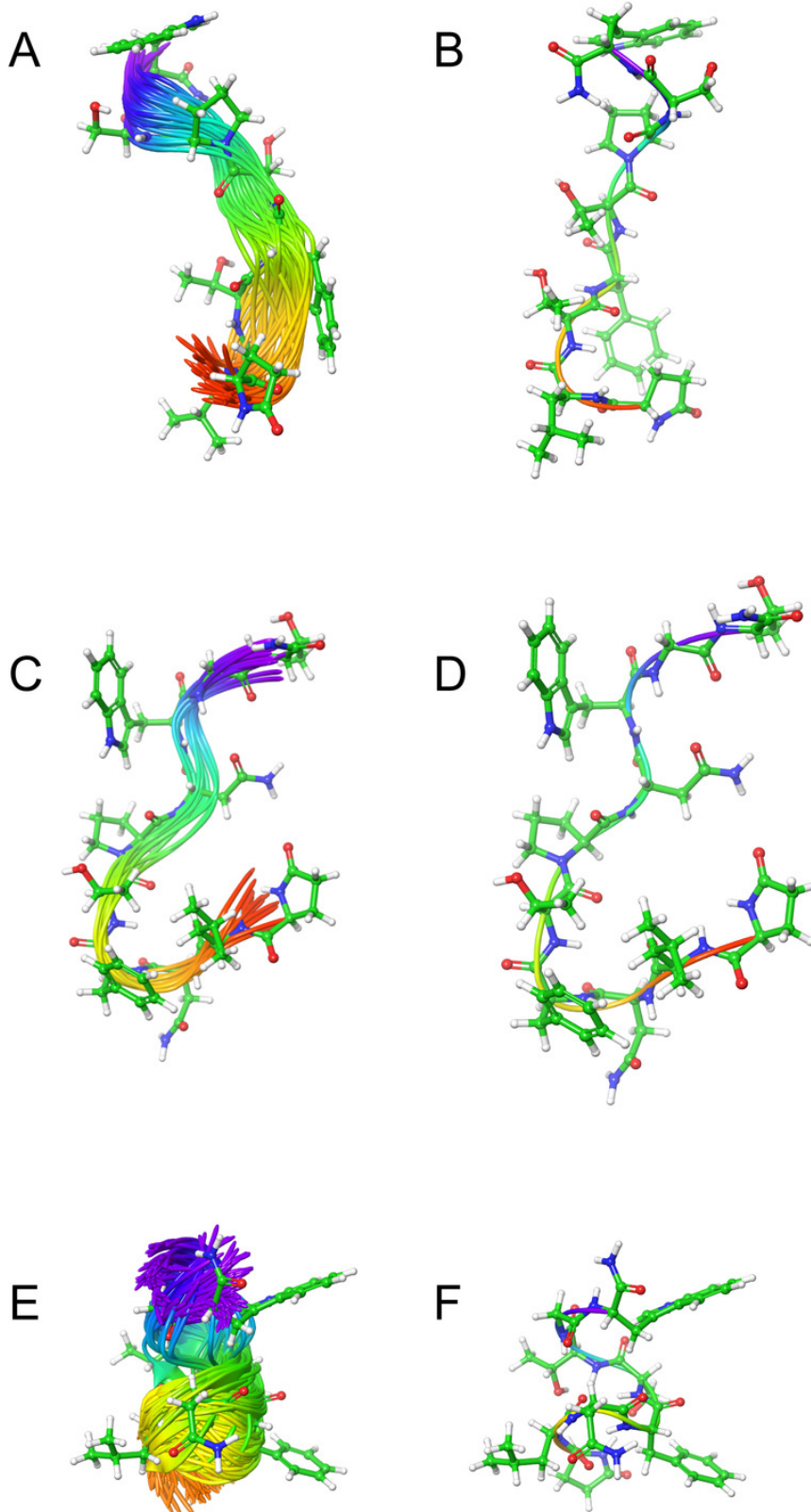
Figure 3

Contact surface area between the peptides and DPC micelle.

Plot of contact area between peptide and a DPC micelle during a 60 ps simulation of Locmi-AKH-I, Aedae-AKH-I and Schgr-AKH-II, as a function of time.
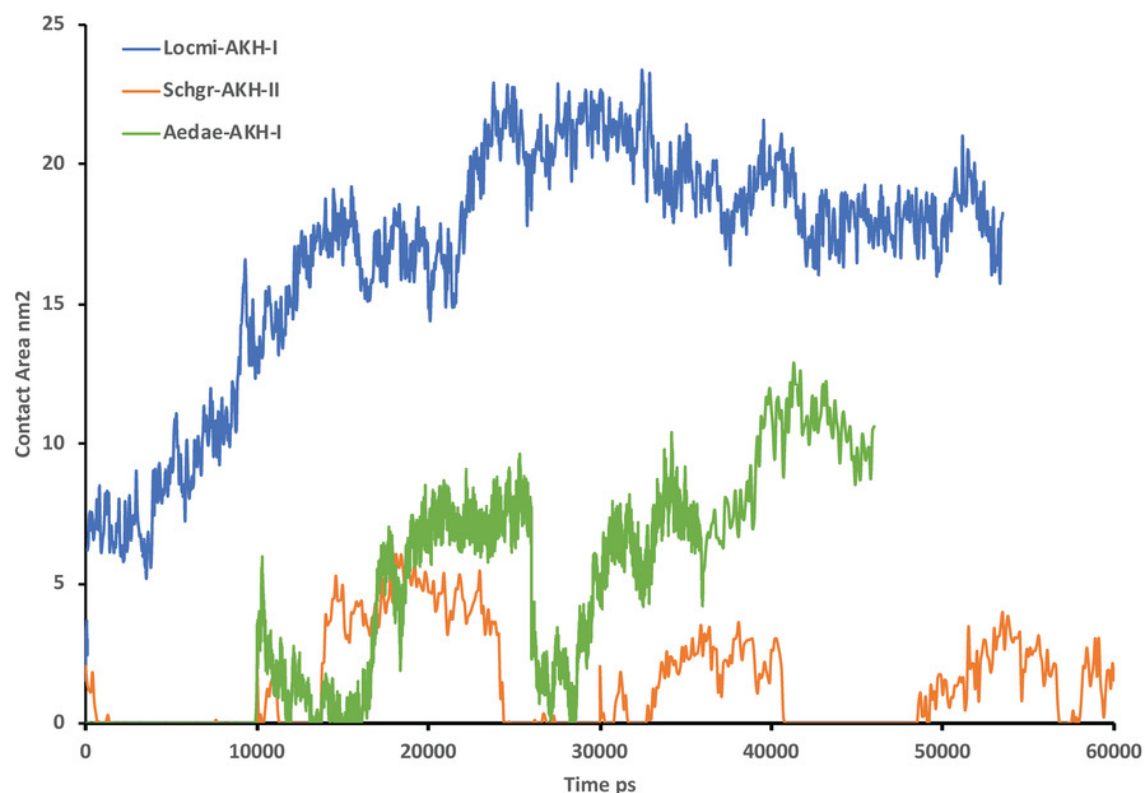
Figure 4

Structure of Schgr-AKH-II in solution and bound to Schgr-AKHR.

(a) Overlay of several snapshots of the dynamic simulation of Schgr-AKH-II in the Schgr-AKH Rreceptor binding pocket. Helices are labelled H1 - 7. (b) Enlargement of binding pocket showing orientation of peptide. Important extracellular loops are labelled. (c) Conformation of bound Schgr-AKH-II. (d) Overlay of best binding pose and root conformer from simulation in DPC micelle solution.
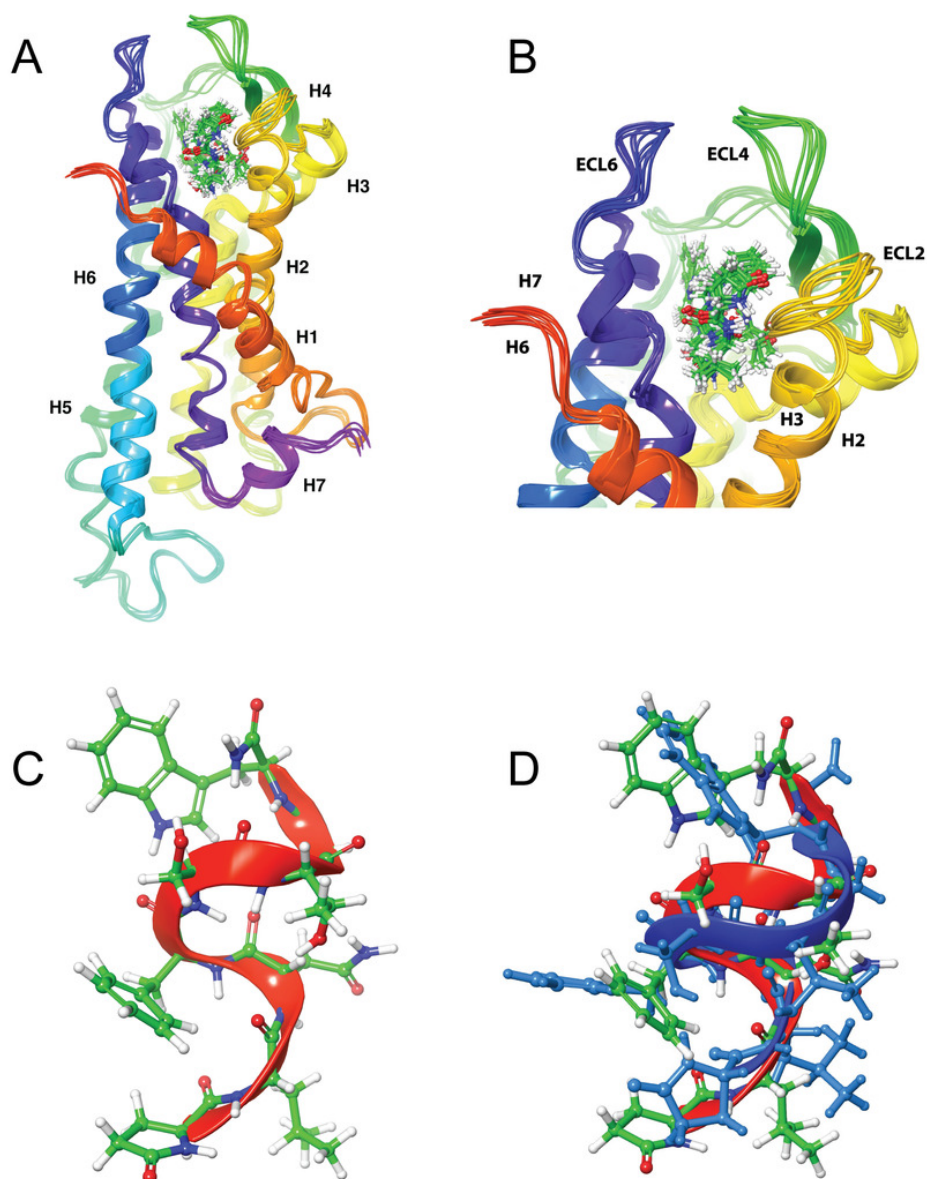
Figure 5

Structure of Locmi-AKH-I in solution and bound to Schgr-AKHR.

(a) Conformer of bound Locmi-AKH-I. (b) overlay of bound Locmi-AKH-I (blue) and in DPC micelle solution. (c) Pictorial representation of Schgr-AKHR with Locmi-AKH-I in the binding pocket. (d) Enlargement of binding pocket showing the orientation of the peptide. (e) Binding pocket surface with Locmi-AKH-I inserted. Surface is coloured according to electrostatic potential, red for negative potential, blue for positive potential and grey for neutral potential.
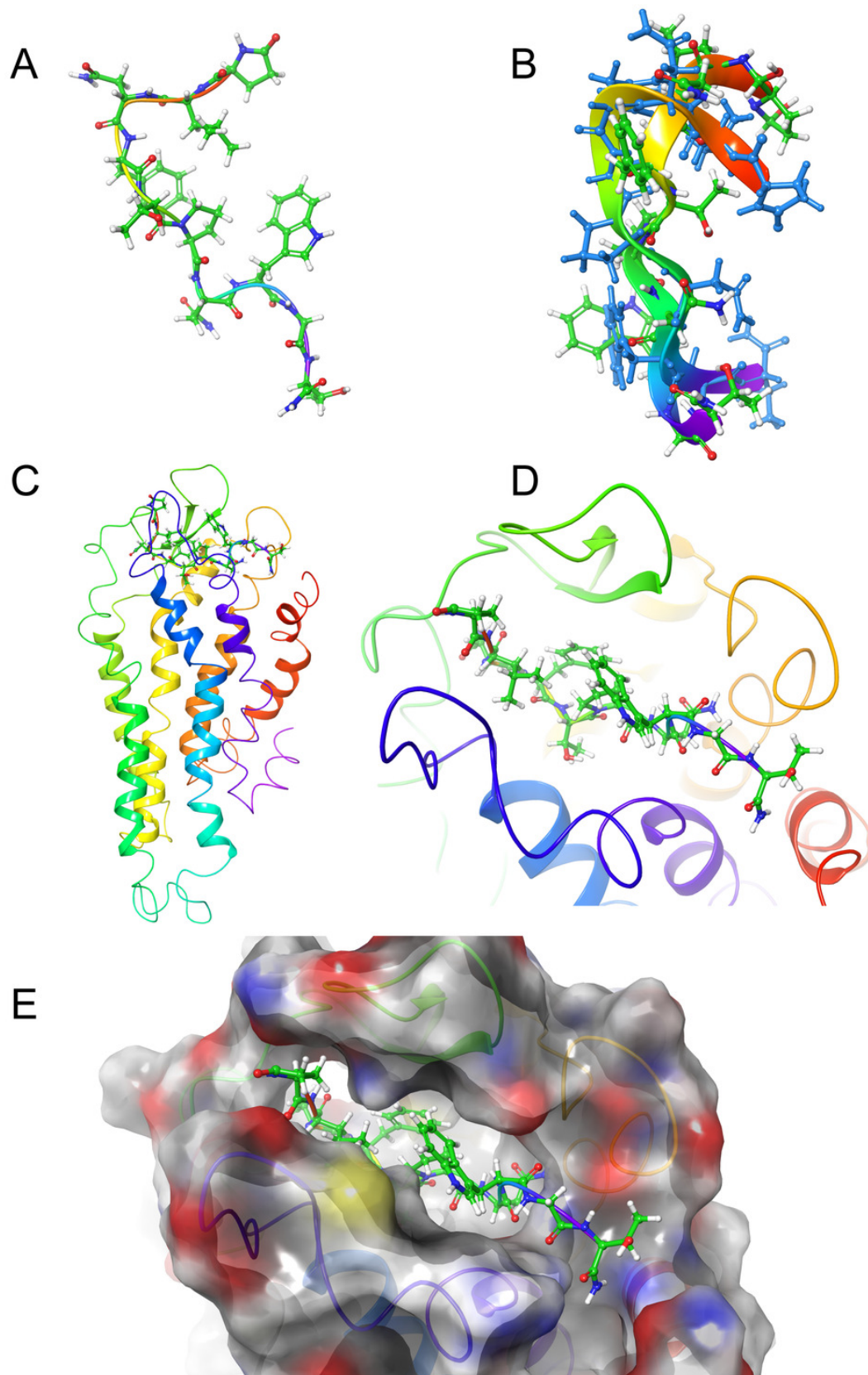
Figure 6

Structure of Aedae-AKH in solution and bound to Schgr-AKHR.

(a) Pictorial representation of Schgr-AKHR with Aedae-AKH in the binding pocket. (b) Enlargement of binding pocket showing the orientation of peptide. (c) Conformer of bound Aedae-AKH. (d) Overlay showing the different conformers of bound Aedae-AKH (blue) and in DPC solution. (e) Binding pocket surface with Aedae-AKH inserted. Surface colored according to electrostatic potential, red for negative potential, blue for positive potential and green for neutral potential.
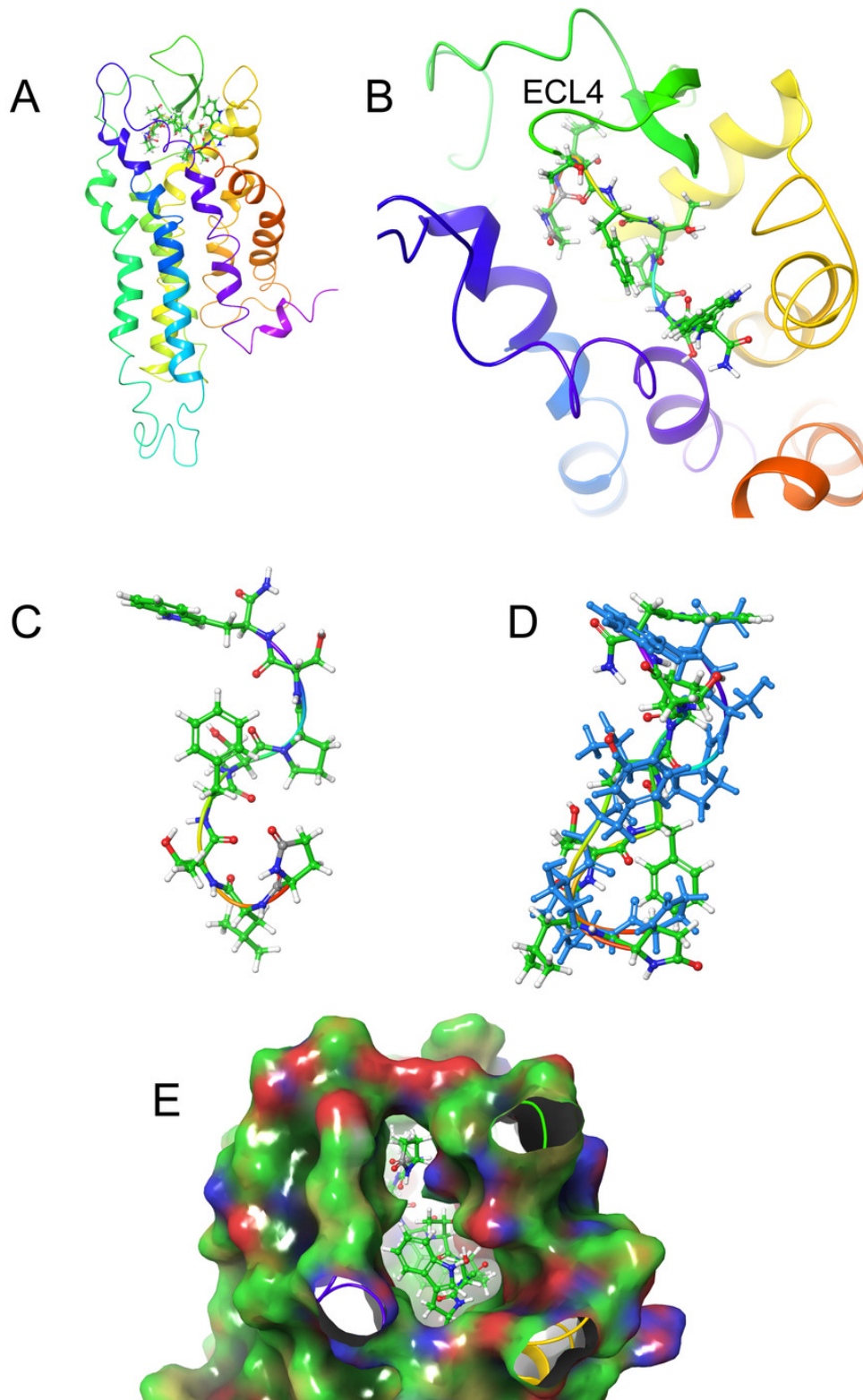
Figure 7

Protein - Ligand interaction diagrams.

(a) Aedae-AKH, (b) Schgr-AKH-II, (c) Locmi-AKH-I. Residues are represented as colored spheres, labeled with the residue name and residue number, and colored according to their properties, green for hydrophobic, blue for positive charge and red for negative charge. The ligand is displayed as a 2D structure. Interactions between the residues and the ligand are drawn as lines, colored by interaction type, purple for H-bonding and green for pi-pi stacking. The binding pocket is indicated by a line drawn around the ligand, colored by the color of the nearest residue. Solvent exposure is indicated on the ligand atoms, and by the break in the line drawn around the pocket.
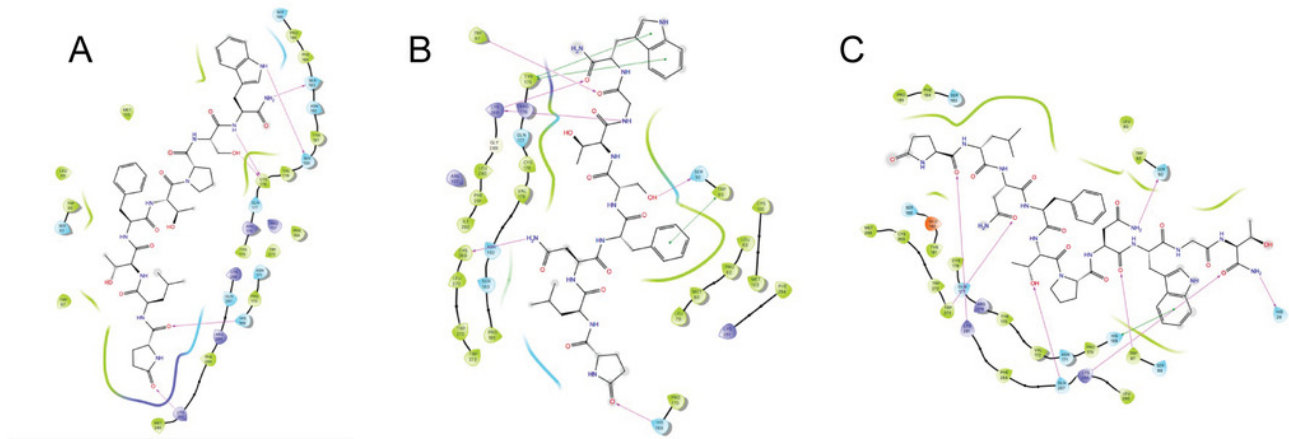
Figure 8

Comparison of active and inactive Schgr-AKH-II receptor.

(a) Overlay of active (colored) and inactive (green) *S. gregaria* receptor. (b) Closed DRY switch. (c) open DRY switch. Only polar hydrogens are shown.
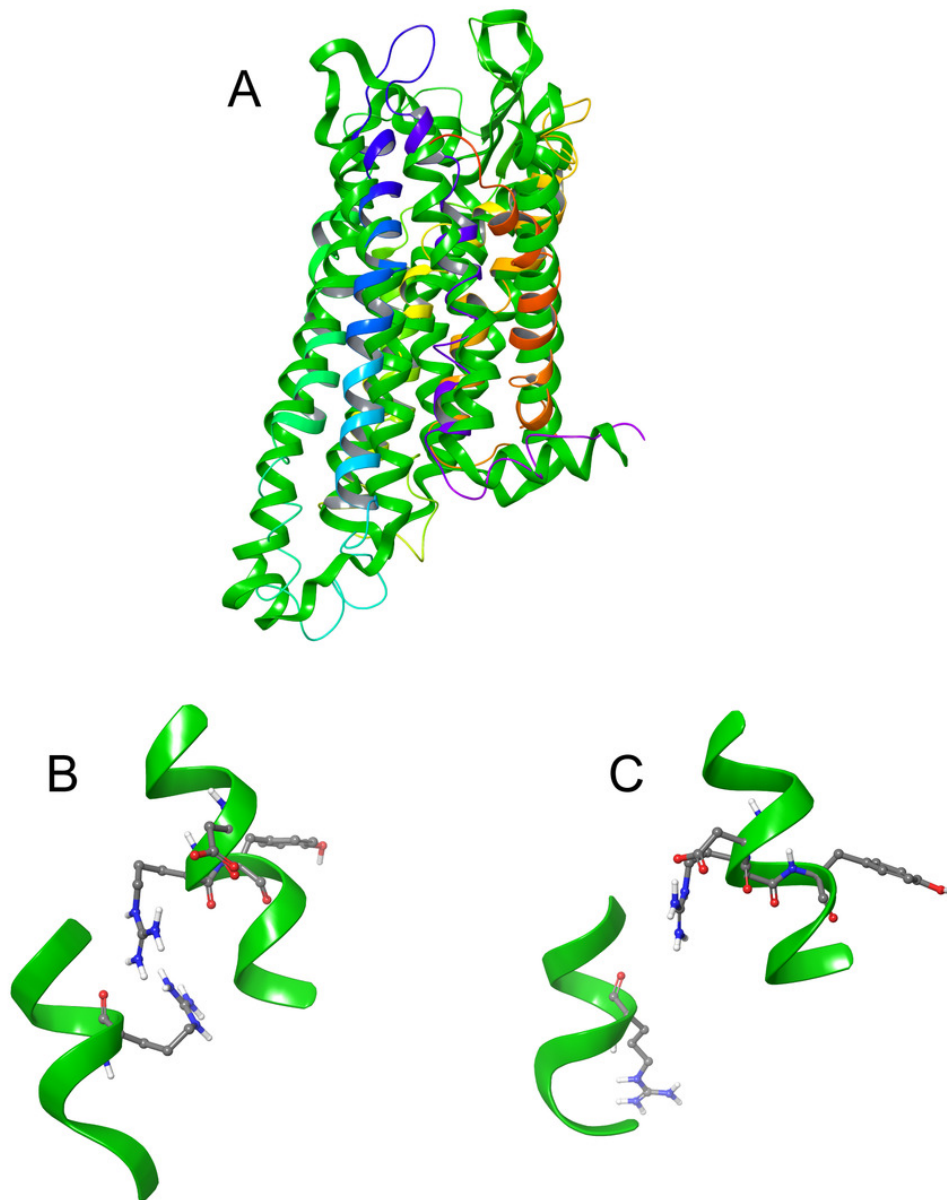
Figure 9

Schgr-AKHR molecular switches of the active and inactive receptor.

(A) TM3-6 lock of inactive receptor. (B) TM3-6 lock of active receptor. (C) Tyrosine toggle switch of inactive receptor. (D) Tyrosine toggle switch of active receptor. (E) CWxPY motif on TM6 of inactive receptor. (F) CWxPY motif on TM6 of active receptor.
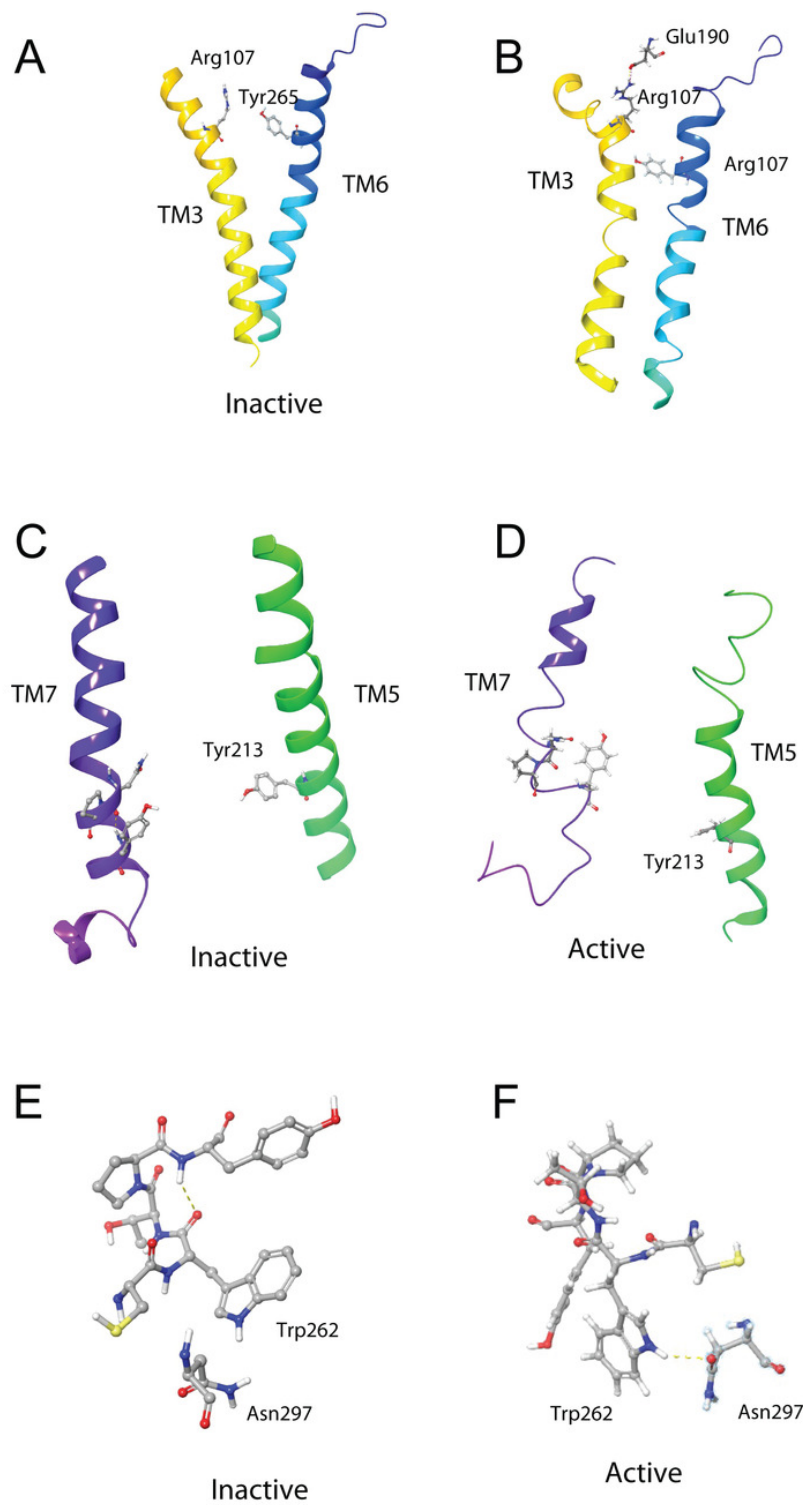
A

Arg107

Tyr265

TM3

TM6

Inactive

B

Glu190

Arg107

TM3

Arg107

TM6

C

TM7

TM5

Tyr213

Inactive

D

TM7

TM5

Tyr213

Active

E

Trp262

Asn297

Inactive

F

Trp262

Asn297

Active

Primary structure of the adipokinetic peptides of locusts. Conserved residues are highlighted in bold and underlined.

1 **Table 1.** Primary structure of the adipokinetic peptides of locusts.   Conserved residues are
2 highlighted in bold and underlined.

3	Peptide name	Sequence	Species
4	Locmi-AKH-I	p**EL**N**F**TPN**W**GT amide	*L. migratoria*; *S. gregaria*
5	Locmi-AKH-II	p**EL**N**F**SAG**W** amide	*L. migratoria*
6	Locmi-AKH-III	p**EL**N**F**TPW**W** amide	*L. migratoria*
7	Locmi-AKH-IV	p**EL**T**F**TPS**W** amide	*L. migratoria, S. gregaria*
8	(= Aedae-AKH)		
9	Schgr-AKH-II	p**EL**N**F**STG**W** amide	*S. gregaria*
10			
11			

^{1}H chemical shifts of Schgr-AKH-II.

A. A. DPC micelle solution, pH 4.5, 20mM phosphate, Temp = 280 K

B. 30% DMSO solution, pH 4.5, 20mM phosphate, Temp = 298 K

1   Table 2. 1H chemical shifts of Schgr-AKH-II:

2   A.   DPC micelle solution, pH 4.5, 20mM phosphate, Temp = 280 K

#	Res	HN	Hα	Hβ (Hβ')	Others
1	Glu	7.742	4.361	2.335,	Hγ:2.483,1.951
2	Leu	8.259	4.232	1.614,1.318	Hδ:0.863
3	Asn	8.364	4.660	2.767,2.647	Hδ:6.864,7.565
4	Phe	7.978	4.561	3.071,2.992	
5	Ser	8.096	4.289	3.782,3.689	
6	Thr	7.923	4.179	3.908	Hγ: 1.040
7	Gly	8.145	3.845,3.905		
8	Trp	7.790	4.587	3.181,3.183	Hδ:7.164, Hε:9.894,7.513, Hζ:7.360,6.959,Hη:7.005

B.   30% DMSO solution, pH 4.5, 20mM phosphate, Temp = 298 K

#	Res	HN	Hα	Hβ (Hβ')	Others
1	Glu	7.770	4.173	2.238,	Hγ:2.361,1.888
2	Leu	8.199	4.160	1.436,1.304	Hδ:0.732,0.780
3	Asn	8.208	4.501	2.519,2.594	Hδ:6.777,7.440
4	Phe	8.077	4.467	3.046,2.849	
5	Ser	8.134	4.318	3.710,3.667	
6	Thr	7.917	4.165	4.076	Hγ:na,1.050
7	Gly	8.132	3.794,3.691		
8	Trp	7.874	4.466	3.187,3.018	Hδ:7.096, Hε:10.111,7.539, Hζ:7.355,7.021,Hη:7.103

^{1}H and ^{13}C chemical shifts of Locmi-AKH-I.

^{1}H and ^{13}C chemical shifts of Locmi-AKH-I in DPC micelle solution at 285 K, a pH of 5.0 and 20 mM phosphate buffer.

1 Table 3 Locmi-AKH-I; pELNTPNWGT-NH2 in DPC solution pH 5.0, Temp = 285K

#	Res	HN	H$_\alpha$ (C$_\alpha$)	H$_\beta$ (H$_{\beta'}$) (C$_\beta$)	Others
1	Glu		4.09	1.642	Hγ:1.541,1.145
2	Leu	8.271	4.32 (54.7)	1.501,1.715 (41.8)	Hγ:1.620,Hδ:0.978,0.964 Cδ1 23.4, Cδ2 25.0
3	Asn	8.491	4.71	2.715,2.806 (38.6)	Hδ:6.871,7.585
4	Phe	7.768	4.67(52.3)	2.984,3.072 (40.3)	Hδ:7.182,Hϵ:7.260,Hζ:7.289 Cδ 131.5, Cϵ 130.8, Cζ 130.6
5	Thr	7.987	4.49 (57.8)	4.015 (69.9)	Hγ:1.080 Cγ2 20.7
6	Pro		4.44 (59.0)	2.031,2.586 (27.8)	Hγ:2.418 Cγ 31.9
7	Asn	8.336	4.68	2.672,2.801 (35.6)	Hδ:6.851,7.563
8	Trp	7.529	4.74	3.301 (29.7)	Hδ:7.247, 7.091,Hζ:7.448,7.617,Hη:7.130 Cδ 126.4, Cϵ 121.1, Cη 123.6, Cζ 113.5, 120.2
9	Gly	8.316	3.94,4.05 (45.3)		
10	Thr	7.988	4.288 (61.5)		Hγ:1.207 Cγ 21.3

¹H chemical shifts of Aedae-AKH.

¹H chemical shifts of Aedae-AKH in DPC micelle solution at 285 K, a pH of 5.0 and 20 mM phosphate buffer.

1   Table 4 Aedae-AKH-I in DPC solution pH 5.0, Temp = 285K

#	Res	HN	HA	HB (HB')	Others
1	Glu		4.41	2.36	Hγ:2.53, 1.962
2	Leu	8.26	4.38	1.47, 1.66	Hγ:1.68, Hδ:0.91, 0.932
3	Thr	8.20	4.33	4.18	Hγ:1.10
4	Phe	7.82	4.66	3.28	Hδ:7.15, Hε:7.22, HZ:7.25
5	Thr	7.96	4.42	3.93	Hγ:1.02
6	Pro		4.42	1.44, 1.56	Hγ:1.97, 2.53, Hδ:3.08, 3.38
7	Ser	8.28	4.25	3.81	
8	Trp	7.82	4.63	2.93, 3.04	Hδ:7.21, Hε:9.99, 7.06, Hζ:7.40, 7.58, Hη:7.09

List of interactions between peptide and receptor in the binding pocket of Schgr-AKHR.

1   Table 5. List of interactions of ligand/receptor in binding pocket of Schgr-AKHR receptor.

Schgr_AKH		Locmi-AKH		Aedae-AKH	
Ligand	Receptor	Ligand	Receptor	Ligand	Receptor
$pE^1O_{\varepsilon1}$	His169	pE^1CO	Lys281	pE^1CO	His169
N^3NH_2	Cys269	N^3CO	Trp273	$pE^1O_{\varepsilon1}$	Lys281
$F^4\pi$-π stack	Trp93	T^5OH	Gln287	S^7OH	Cys178
S^5OH	Ser92	N^7CO	Trp87	S^7NH	Cys178
G^7NH	Lys288	N^7NH_2	Ser92	$W^8 H_{\varepsilon1}$	Ser180
G^7CO	Trp87	$T^{10}CO$	Lys288	W^8NH_2	Ser183
W^8CO	Lys288	$W^8 \pi$-π stack	His169		
$W^8\pi$-π stack	Tyr175	$T^{10}NH_2$	His28		